ISSN 0208-7774 TRIBOLOGIA 5/2020 p. 73–84
DOI: 10.5604/01.3001.0014.6961

Stanisław STRZELECKI *

EFFECT OF THE MISALIGNMENT OF JOURNAL AND SLEEVE AXIS ON THE OPERATION OF TURBO UNIT JOURNAL BEARINGS

WPŁYW NIEWSPÓŁOSIOWOŚCI OSI CZOPA I PANEWKI NA PRACĘ ŁOŻYSK ŚLIZGOWYCH TURBOZESPOŁU

Key words: hydrodynamic lubrication, multilobe journal bearings, oil film temperature.

Abstract: In journal bearings the misalignment of the journal and sleeve axis causes a load concentration on their edges, mixed lubrication conditions, an increase in the bearing temperature, rotor instability, and intensive wear of mating parts. The rotating machines are controlled by means of the temperature and vibration transducers, which are placed in the middle plain of the bearing housing. This arrangement of transducers gives no information about the real distance between the journal surface and bearing edges, and, in case of misaligned shaft, it has crucial meaning for the correct operation of turbo unit.
This paper presents the theoretical and some experimental results of turbo unit journal bearing operating in misaligned conditions. The results point out the necessity of the precise control of the lubricating gap and the temperature generated on the bearing edges. It was also found that the increase in misalignment also generates an increase in power loss.

Słowa kluczowe: smarowanie hydrodynamiczne, wielopowierzchniowe łożyska ślizgowe, temperatura filmu smarowego.

Streszczenie: W warunkach niewspółosiowości osi czopa i panewki w łożysku występuje koncentracja nacisków na jego krawędziach, tarcie mieszane oraz zwiększone zużycie i niestateczna praca. W maszynie wirnikowej temperatura pracy łożysk oraz ich drgania kontrolowane są czujnikami umieszczonymi w płaszczyźnie środkowej obudowy łożyska. Brak jest danych o rzeczywistej odległości między powierzchnią ślizgową łożyska i jego krawędziami. W przypadku niewspółosiowości takie informację są bardzo ważne dla prawidłowej pracy turbozespołu.
Wyniki badań teoretycznych oraz pomiarów przemieszczeń na rzeczywistym obiekcie, jakim jest turbozespół wskazują na konieczność sprawdzania temperatury na krawędziach łożysk. Wzrost niewspółosiowości osi czopa i panewki powoduje m.in. wzrost strat mocy.

INTRODUCTION

The problems of misalignment exist, at present, in journal bearings, and they have a considerably effect on the static and dynamic characteristics of rotating machines **[L. 1–7]**. It could cause faster wear of the bearing, vibration, and even failure of the bearing system. Theoretical and experimental investigation into the performances of misaligned and statically loaded cylindrical journal bearings has revealed the asymmetrical distribution of oil film pressure and temperature **[L. 3, 8]**. The investigation into the misalignment concentrate, among others, on the influence of thermal effects **[L. 4, 6]**, the flexibility of supports and compliant liners **[L. 9, 10]**, the texture surface **[L. 11]**, and the axial profile of sleeve **[L. 5].** The effect of the axial movement of misaligned journal in the bearing with rough surface and angular misalignment were investigated in **[L. 12, 13**]. A new method for the analysis of a misaligned bearing comprising three-dimensional misalignment geometry is given in **[L. 14]**. The wear process generated by misalignment was described in **[L. 2]** and can be identified by application of artificial neural networks **[L. 15].**

ORCID: 0000-0001-5030-5249.

The bearings of large multistage turbogenerators have a basic effect on the reliability and durability of these machines **[L. 2, 4]**. The main task of these, mainly 2- and 3-lobe journal bearings **[L. 2]**, is to assure the operation of turbo units at the assumed temperature and minimum power loss, the correct vibration frequency of shafts line, and the largest resistance against the accidental external loads that cause the unstable behaviour of the rotor. Fulfilling these tasks is very important for both the designer and the operator of the rotating machinery.

The demands of power industry are for very durable and reliable turbo units, which fulfil simultaneously the requirements of the shortest time of overhaul and maintenance **[L. 2]** to assure their maximum disposability. There is the need of the analysis of factors affecting the operation of bearings system, e.g., misalignment as well as considering these factors in the existing or new methods of calculations **[L. 10, 14]**.

Large turbogenerators have a multistage turbine and generator, which often are manufactured by different companies, and they are assembled by means of the stiff couplings into one whole unit, operating through a long period of time. The single members of this unit **[L. 2]** or, e.g., the marine propulsion shafting **[L. 9]**, interact with other members of the unit, as observed during the operation of journal bearings **[L. 2, 9]**. These elements of the generator as well as some design solutions of turbogenerators are similar to machines with the shaft supported in two points. The loads applied to the bearings are considered as static and their calculations are carried out as a two-step procedure. In the first step, the value of applied external load is used for the calculation of static characteristics which comprise the static equilibrium position angles, the minimum oil film thickness, the maximum oil film pressure and temperature, oil flow, and power loss. The second step determines the stiffness and damping coefficients, which are used for the calculation of critical speeds and the stability of the rotor **[L. 2, 3]**.

The displacements of turbo units are very complex and can be investigated experimentally or theoretically as calculation models. During the operation of such models, there are cases of the incorrect reaction of the control unit at the correct technical state of journal bearings. In some cases, the control system failed causing the danger of bearing damage (e.g., an excessive wear of bearings were observed) **[L. 2, 15]**. The information from the control system indicate the displacements of bearing pedestals, causing the change in the shaft position and an increase in vibrations level; however, the level of vibration may not increase to a dangerous level.

Some reasons for the incorrect operation of the control system of vibration explain the misaligned orientation of the journal and bearing axis. The position of temperature and vibration transducers in the middle plain of the bearing is under a question. Misalignment causes asymmetrical oil film pressure and temperature distribution, and their excessive values can be the reason of weakening of bearing material and the damage of bearing **[L. 2, 10]**.

In the presented paper, the bearing system of a multistage shaft line of a turbogenerator is characterised. The real conditions of the bearing operation and the relation to the calculation model of bearings are introduced. Theoretical calculations of 2-lobe journal bearings were carried-out on the assumption of adiabatic oil film, the static equilibrium position of journal, and the misaligned orientation of the journal and bearing axis.

BEARINGS SYSTEM OF SHAFT LINE

There are different bearing systems of shaft lines of turbo units **[L. 3, 4]**; however, the solution showed in **Fig. 1** is applied in practice. The difference in the turbo unit bearings system consists in the number of bearings, their positioning, and the way of coupling of single shafts. These factors have an effect on the load of single bearing and the line of shaft deflection as well as on the value of the misalignment of journal and bearing axis. The system of shafts line creates the beam supported in many points, i.e. the static indeterminable system. The values of reactions at the supports are calculated statically for a stationary shaft. During operation (**Fig. 1** – hot state) of turbo unit, the shaft rotates and the deflection of shaft line differs from its static deflection line, which causes the variation of bearings load. The variation of the shaft's deflection line at the different states of turbo unit

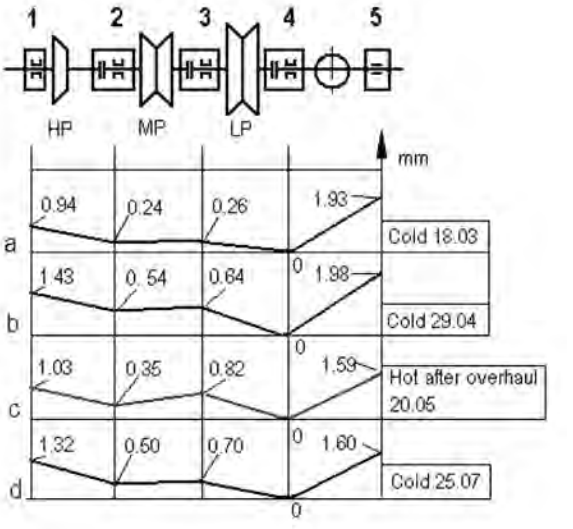

Fig. 1. Variation of the deflection line of shafts at different states of turbo unit rotor operation; HP, MP, LP – high, medium and low pressure parts of turbine, 1, 2, 3, 4, 5 – journal bearings numbers [L. 2]

Rys. 1. Odkształcenia linii wałów w różnych stadiach pracy turbozespołu; HP, MP, LP – wysoko-, średnio- i niskoprężny stopień turbiny, 1, 2, 3, 4, 5 – numery łożysk ślizgowych **[L. 2]**

operation, i.e. in case of cold or hot state of operation is presented in **Fig. 1**. The differences in shaft line at the cold or hot operation certifies that real bearings system operates in the conditions of a misaligned axis of the journal and sleeve.

The displacements of bearings supports produce heat, deformations of bearings housings and the foundation, which are observed during operation **[L. 6, 8]** of the turbo unit, and they cause the changes of shaft static line and the values of load applied to the bearings. The dynamic state of machine, the method of turbo unit assembly, the unbalance of rotating parts, incorrect connections of turbo unit elements are also reasons for additional bearings loads which generate the vibrations affecting the operation of bearings **[L. 2, 4]**.

The asymmetric oil film pressure and temperature distributions in the axial direction that are caused by the misalignment of journal and bearing axis change the position of oil film resultant force and affect the static deflection line of the shaft as well as the bearing static **[L. 4, 12]** and dynamic characteristics as compare to the parallel orientation of the journal and bearing axis **[L. 2, 3]**.

GEOMETRY AND HYDRODYNAMIC EQUATIONS OF THE BEARING OPERATING WITH MISALIGNED AXIS

The general geometric position of the shaft in the journal bearing can be reduced to the tilt in two different planes that are at right angles to each other. For the special case of a single external force, the inclination plane of the shaft coincides with the load plane, and this case **[L. 2, 8]** was considered in this paper.

In very many cases, the useful load of the turbine rotor is supported between two journal bearings. As a result, the shaft axis is then slightly bent and is no longer parallel to the axis of the bearing **[L. 4, 8]**. Non-parallelism causes the minimum oil film thickness is at the edges of the bearing. It explains why such bearings tend towards increased edge loading with greater wear during the running-in period. The bending of the shaft

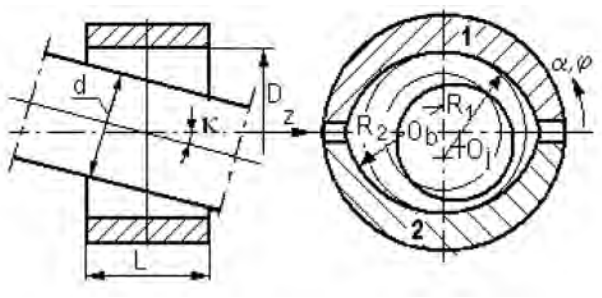

Fig. 2. Geometry of misaligned bearing; $R_{1,2}$ – radii of segments, O_b, O_j – centre of bearing and journal

Rys. 2. Geometria łożyska z niewspółosiowością; $R_{1,2}$ – promienie segmentów, O_b, O_j – środek łożyska i czopa

depends on the force applied as well as on its rigidity and length, and a general bending parameter is defined which results from the respective shaft dimensions, supporting lengths, and forces.

The geometry of the multi-lobe journal bearings with misaligned axis **[L. 2, 6]** is described by Eq. (1) and is shown in **Fig. 2**. The oil film geometry is distorted by the non-parallel position of the shaft and bearing, and the angular displacement of the shaft with respect to the bearing is described by the Eq. (4).

$$\bar{H}(\varphi, z) = \bar{H}_c + \bar{H}_M(\varphi) + \bar{H}_m(z) \tag{1}$$

The respective terms of the right side of above equation are described by Eq. (1) through Eq. (4). The oil film thickness for the cylindrical journal bearing is from Eq. (2).

$$H_C = 1 - \varepsilon \cdot \cos(\varepsilon - \alpha), \tag{2}$$

where: ε – eccentricity, φ – peripheral co-ordinate, α – attitude angle.

The concentric position of the journal in the sleeve the geometry of multi-lobe bearing is described by Eq. (3).

$$\bar{H}_M(\varphi) = \psi_S + (\psi_S - 1) \cdot \cos(\varphi - \gamma) \tag{3}$$

with ψ_S – segment clearance ratio ($\psi_S = \bar{H}_{max} / \bar{H}_{min}$), γ – peripheral co-ordinate of the segment centre.

Equation (4) gives the correction of the oil film thickness for the misaligned axis of journal and sleeve.

$$H_m(z) = q \cdot z \cdot \cos(\varphi - \alpha), \tag{4}$$

where q – inclination ratio, z – co-ordinate in the axial direction.

Where:

$$q = \frac{L \cdot \tan\kappa}{\Delta d} \quad \text{and} \quad \bar{z} = \frac{z}{L/2} \tag{5}$$

Δd – diametric bearing clearance, $\Delta d = D - d$, d, D – journal and sleeve diameter [m], φ – peripheral coordinate (°), α – attitude angle (°), $\bar{z}$ – dimensionless axial coordinate, z = axial coordinate (m), L – length of bearing (m), κ – inclination angle (°).

The oil film pressure, temperature, and viscosity fields were obtained from Reynolds, energy and viscosity equations on the assumption of laminar adiabatic oil flow through the bearing gap **[L. 2, 8]**. The Reynolds equation that was applied in this paper has the following form:

$$\frac{\partial}{\partial\varphi}\left(\frac{\bar{H}^3}{\bar{\eta}}\frac{\partial\bar{p}}{\partial\varphi}\right)+\left(\frac{D}{L}\right)^2\frac{\partial}{\partial\bar{z}}\left(\frac{\bar{H}^3}{\bar{\eta}}\frac{\partial\bar{p}}{\partial\bar{z}}\right)=6\frac{\partial\bar{H}}{\partial\varphi}+12\frac{\partial\bar{H}}{\partial\phi}, \tag{6}$$

where D, L – bearing diameter and length (m), $\bar{H}$ = h/(R-r) – dimensionless oil film thickness, h – oil film thickness (μm), $\bar{p}$ – dimensionless oil film pressure, $\bar{p}$ = $p\psi^2/(\bar{\eta}\omega)$, p – oil film pressure (MPa), r, R – journal and sleeve radius (m), ϕ, $\bar{z}$ – peripheral and dimensionless axial co-ordinates, φ – dimensionless time, φ = ω t, t – time (sec), ω – angular velocity (sec^{-1}), $\bar{\eta}$ – dimensionless viscosity, ψ – bearing relative clearance, ψ = ΔR/R (‰), ΔR – bearing clearance, ΔR = R-r (m).

It was assumed that, on the bearing edges and in the regions of negative pressures, the oil film pressure is nil, i.e. p(φ, $\bar{z}$) = 0 or different from this value. The oil film pressure obtained from Eq. (3) was put into energy equation, thus allowing the calculation of the oil film temperature and viscosity distributions **[L. 6, 8]**.

The viscosity was described by exponential equation **[L. 8]**. Oil film temperature and viscosity distributions have been found by iterative solution of Equations (1) through (6) and energy Eq. (7) **[L. 4, 8]**. Temperature values Tφ, z) on the boundaries ($\bar{z}$ = ±1) were determined by means of the parabolic approximation **[L. 4]**.

$$\frac{\bar{H}}{Pe}\left[\frac{\partial^2\bar{T}}{\partial\varphi^2}+\left(\frac{D}{L}\right)^2\frac{\partial^2\bar{T}}{\partial\bar{z}^2}\right]+\left[\frac{\bar{H}^3}{12\bar{\eta}}\frac{\partial\bar{p}}{\partial\varphi}-\frac{\bar{H}}{2}\right]\frac{\partial\bar{T}}{\partial\varphi}+\left(\frac{D}{L}\right)^2\frac{\bar{H}^3}{12\bar{\eta}}\frac{\partial\bar{p}}{\partial\bar{z}}\frac{\partial\bar{T}}{\partial\bar{z}}= \tag{7}$$
$$=-\frac{\bar{H}^3}{12\bar{\eta}}\left[\left(\frac{\partial\bar{p}}{\partial\varphi}\right)^2+\left(\frac{D}{L}\right)^2\left(\frac{\partial\bar{p}}{\partial\bar{z}}\right)^2\right]-\frac{\bar{\eta}}{\bar{H}}$$

where: $\bar{T}$ – dimensionless oil film temperature, $\bar{T} = T/T_0$, Pe – Peclet number, $Pe = \rho c\omega r^2/\lambda$, ρ: oil density, ($kg/m^3$), c_t: oil specific heat, (J/kgK), λ – heat transfer coefficient (W/m^2K).

The developed program of numerical calculation **[L. 4]** solves all above-mentioned equations.

RESULTS OF THE INVESTIGATION OF DISTURBANCES IN OPERATION OF TURBOGENERATOR JOURNAL BEARINGS

In one of the turbo units operating in the heat and power generating plant, it was stated that there is an increase in the temperature of 2-lobe journal bearing above the permissible value **[L. 2, 4]**. This bearing's unusual operation has occurred after the main overhaul, and within 3 days of starting trials of the turbo unit. After the first synchronisation and test operation, the temperature of bearing No. 3 (**Fig. 3**), placed between the low (LP) and medium pressure stage (MP), was 92/81°C. After 9 days of operation, this turbo unit was shut-off as result of protection activation. The increase in the bearing temperature (rear part) up to 104°C has occurred during operation under load. After restarting of turbo unit and after reaching the speed 3000 rpm, the temperature of this bearing increased up to 117°C. At the decrease in revolutions down to 2000 rpm, the bearing temperature was 80°C. An increase in the speed up to 3000 rpm again caused the increase of temperature up to 115°C with further tendency in its increase. The temperature of oil on the outflow from this bearing was 51°C. The control of the bearing indicated the marks of sparking between the shaft and external sealing segments in LP part on the side of M. The turbo unit was stopped at the bearing temperature about 117°C. After the run-out of the turbine, the temperature of the considered bearing dropped to about 60°C. For the purpose of explaining this problem, the speed of turbine was increased again up to 3000 rpm, and the increase in the bearing temperature was up to 120°C (from the low pressure LP side). After 30 minutes of operation, the turbo unit was synchronised with the power network; however, but on the side of Bearing No.3, the sparking occurred on the LP sealing. After the next 30 minutes of operation, the protection was activated and a quick increase in bearing temperature was observed with oscillations up to 140°C. As a result of this temperature problem, the turbo unit was shut-off. After a cooling procedure, the observations were made of bearing No. 3 and the external packings of low pressure LP.

As a result of these observations, the following can be stated:

1. For Bearing No. 3, the following were noted:
   – There was partial melting of bearing material in the bottom half from the low pressure LP side. The width of melted part was about 230 mm and the depth 0.07 mm along the bearing axis, and the

melted material was observed on the operating surface of bottom half of bearing and partially was transferred to the lubricating pocket.
– There was vertical displacement (inclination) of MP/LP (**Fig. 3**) pedestal with regard to the position in cold state after the overhaul.

2. For external packings of the low pressure LP part, the following was noted:
   – After opening of the upper covers of sealing of low pressure LP (rear and face) side, an asymmetrical orientation of value 0.38 mm on the left side, with respect to the shaft axis in the parting plane, was observed.

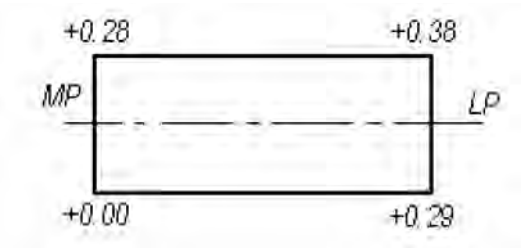

Fig. 3. Measured displacements of bearing pedestal No. 3 (MP – mean pressure part, LP – low pressure part; values of displacements in μm) [L. 2]

Rys. 3. Zmierzone przemieszczenia podpory łożyskowej nr 3 (MP – część turbiny o średnim ciśnieniu, LP – część niskociśnieniowa; wartości przemieszczeń w μm) **[L. 2]**

The measurements indicate the inclination of the journal and bearing axis (**Fig. 2**) **[L. 2]**.

RESULTS OF THEORETICAL INVESTIGATION

In the theoretical investigation, the 2-lobe journal bearings with the aspect ratio L/D = 0.5, L/D = 0.8, L/D = 0.88 and L/D = 1.0 have been considered **[L. 2, 8]**. The following bearing static characteristics were determined at different values of misalignment coefficient q:

1) oil film temperature distributions in axial cross-sections of bearing that were placed in four different points of bearing peripheral (**Fig. 9** through **Fig. 12**); and,
2) the contour lines of dimensionless oil film thickness and isobars of oil film pressure (**Fig. 4** through **Fig. 7**), static load capacity, and the angles of static equilibrium position α_{eq} (**Fig. 14**), maximum oil film temperature T_{max} (**Fig. 15**), oil flow q_{flow} (**Fig. 16a**), and power loss P_{loss} (**Fig. 16b**).

It can be observed from **Table 1** and **Table 2** that an increase in misalignment has caused an increase in maximum value of oil film pressure and temperature and the decrease in minimum oil film thickness.

Figures 4 through 7 show some results of the calculations of oil film thickness and pressure in the form of contour lines and isobars, respectively, on the bottom half of 2-lobe bearing and for the case of parallel (q = 0.0 – **Fig. 4** and **Fig. 6**) and nonparallel (q = 0.1 – **Fig. 5** and **Fig. 7**) axis of journal and sleeve. The misalignment changes the contour lines and isobars (the ranges of pressure values are: 6–8 MPa at q = 0.0 and 8–10 MPa at q = 0.1).

Fig. 8 presents the effect of misalignment on the oil film pressure distribution in the axial cross-section on the bottom half of bearing and for two coordinates on the bearing peripheral. Larger misalignment moves the peak of pressure in the direction of bearing edge (q = 0.35 and φ = 2700).

Table 1. Some of the results of the theoretical calculations of bearing with L/D = 1.0 and the relative eccentricity of journal ε = 0.6, bearing relative clearance ψ = 1.5‰ and lobe relative clearance ψ_s = 1.00 [L. 2, 8]

Tabela 1. Przykładowe wyniki obliczeń teoretycznych łożyska przy L / D = 1,0 i względnej mimośrodowości czopu ε = 0,6, luzu względnego łożyska ψ = 1,5 ‰ i luzu względnego płata ψ_s = 1,00 **[L. 2, 8]**

Bearing parameter	Misalignment coefficient q		
	0.0	0.05	0.1
So [–]	0.301	0.358	0.452
α_{eq} [°]	355.4	347.6	343.3
H_{min} [–]	0.688	0.537	0.427
p_{max} [–]	0.701	0.863	1.119
T_{max} [°C]	63.4	72.7	88.4
T_{mean} [°C]	51.1	51.8	53.2

L/D = 1.0, ψ = 1.5‰, ψ_s = 1.00

Remarks: α_{eq} – static equilibrium position angle, H_{min} – minimum oil film thickness, p_{max} – maximum oil film pressure, T_{mean}, T_{max} – mean and maximum temperature of oil film.

Uwagi: α_{eq} – kąt statycznego położenia równowagi, H_{min} – minimalna grubość filmu smarowego, p_{max} – maksymalne ciśnienie w filmie smarowym, T_{mean}, T_{max} – średnia i maksymalna temperatura filmu smarowego.

Table 2. Some calculated values of the turbo unit bearing for different misalignment coefficients q [L. 2]

Tabela 2. Przykładowe wyniki obliczeń parametrów łożyska turbozespołu dla różnych współczynników niewspółosiowości q **[L. 2]**

ε	q [–]	α_{eq} [°]	So [–]	H_{min} [–]	p_{max} [–]	T_{max} [°C]
0.6	0.0	352.40	0.27178	0.670	0.657	61.95
0.6	0.1	337.45	0.42680	0.391	1.136	91.37
0.6	0.15	328.67	0.57538	0.240	1.681	150.34

L/D = 0.88, ψ = 1.5‰, ψ_s = 1.00

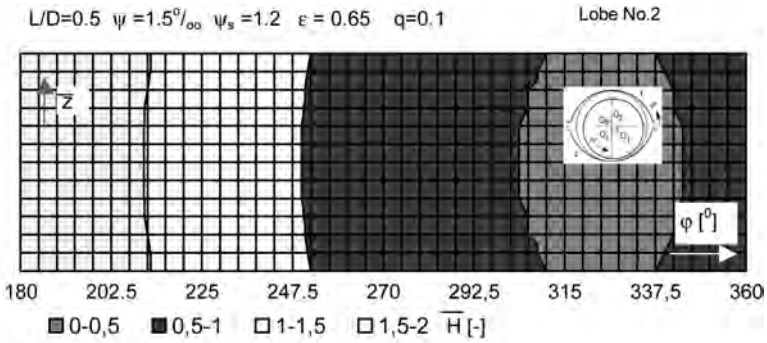

Fig. 4. Contour lines of dimensionless oil film thickness on the bottom half of 2-lobe bearing – no misalignment
Rys. 4. Warstwice bezwymiarowego rozkładu grubości filmu smarowego na dolnej połowie łożyska 2-powierzchniowego – współosiowość osi czopa i panewki

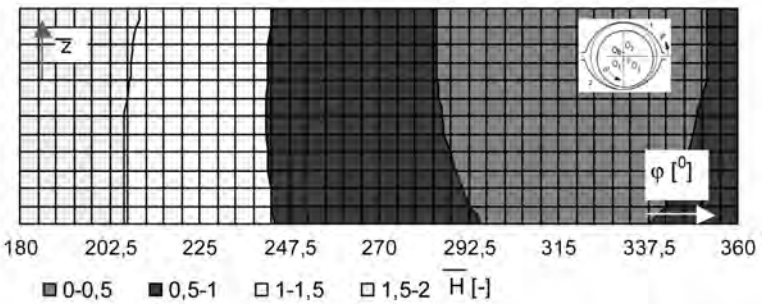

Fig. 5. Contour lines of dimensionless oil film thickness on the bottom half of 2-lobe bearing – misalignment
Rys. 5. Warstwice bezwymiarowego grubości filmu smarowego na dolnej połowie łożyska 2-powierzchniowego – niewspółosiowość osi czopa i panewki

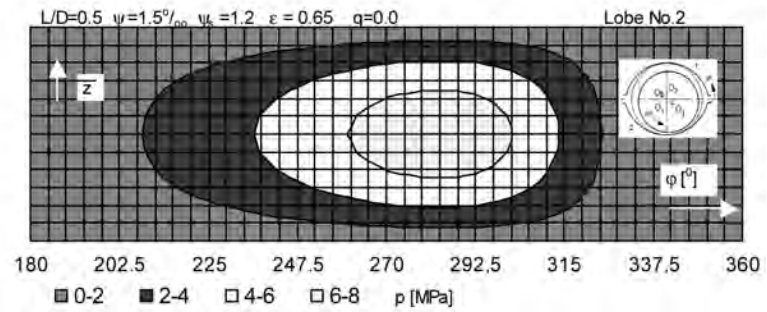

Fig. 6. Isobars of dimensionless oil film pressure on the bottom half of 2-lobe bearing – no misalignment
Rys. 6. Izobary bezwymiarowego rozkładu ciśnienia na dolnej połowie łożyska 2-powierzchniowego – współosiowość osi czopa i panewki

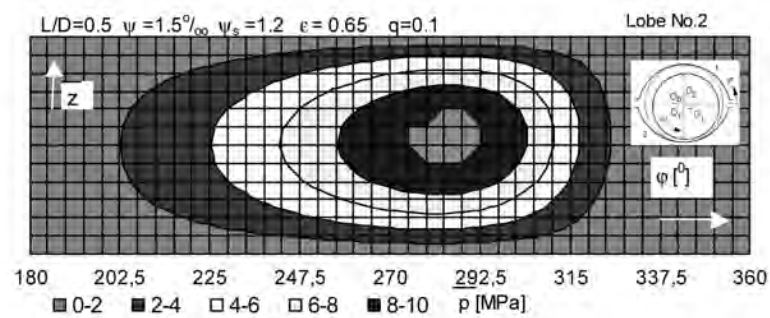

Fig. 7. Isobars of dimensionless oil film pressure on the bottom half of 2-lobe bearing- misalignment
Rys. 7. Izobary bezwymiarowego rozkładu ciśnienia na dolnej połowie łożyska 2-powierzchniowego – niewspółosiowość osi czopa

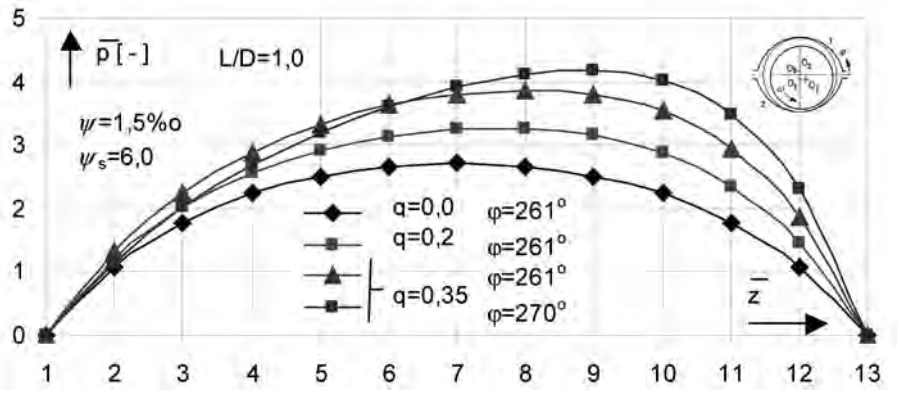

Fig. 8. Oil film pressure distribution in the axial cross-section on the bottom half of 2-lobe bearing with misaligned axis of journal and sleeve for different values of misalignment coefficients and peripheral coordinates

Rys. 8. Rozkłady ciśnienia w przekroju wzdłużnym na dolnej połowie łożyska 2-powierzchniowego dla niewspółosiowych osi czopa i panewki dla różnych współczynników niewspółosiowości i współrzędnych obwodowych

Figures 9 through **12** present the oil film temperature distributions in axial cross-section of bearing versus axial coordinates for assumed relative eccentricity ε at different bearing relative clearance (ψ = 1.5‰, b – = 2.5‰), four values of peripheral coordinates, length to diameter ratios L/D = 0.5, L/D = 0.8 and L/D = 1.0 without and with misalignment coefficient q = 0.2. The misalignment generates the asymmetrical run of temperatures in axial distributions of oil film temperatures with the highest temperature occurring close to the edge of lobe No .2 (e.g., **Fig. 9a**, **Fig. 11** and **Fig. 12b** at φ = 355.5^0). **Figure 10** shows the changes of the temperatures of the bearing with L/D = 0.8 that are caused by the changes in bearing relative clearance but without misalignment; an increase in the clearance decreases the values of temperatures (**Fig. 10a** and **Fig. 10b**).

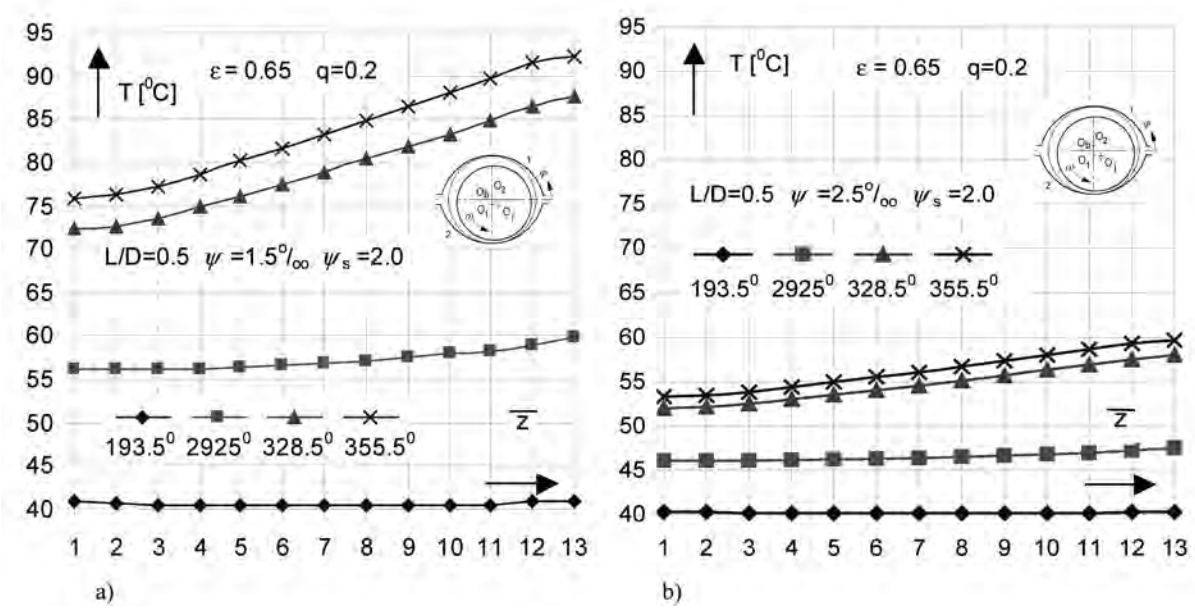

Fig. 9. Oil film temperature in axial cross-section at different bearing relative clearance and misalignment q = 0.2

Rys. 9 . Temperatura filmu smarowego w przekroju wzdłużnym dla różnego luzu łożyskowego i niwspółosiowości

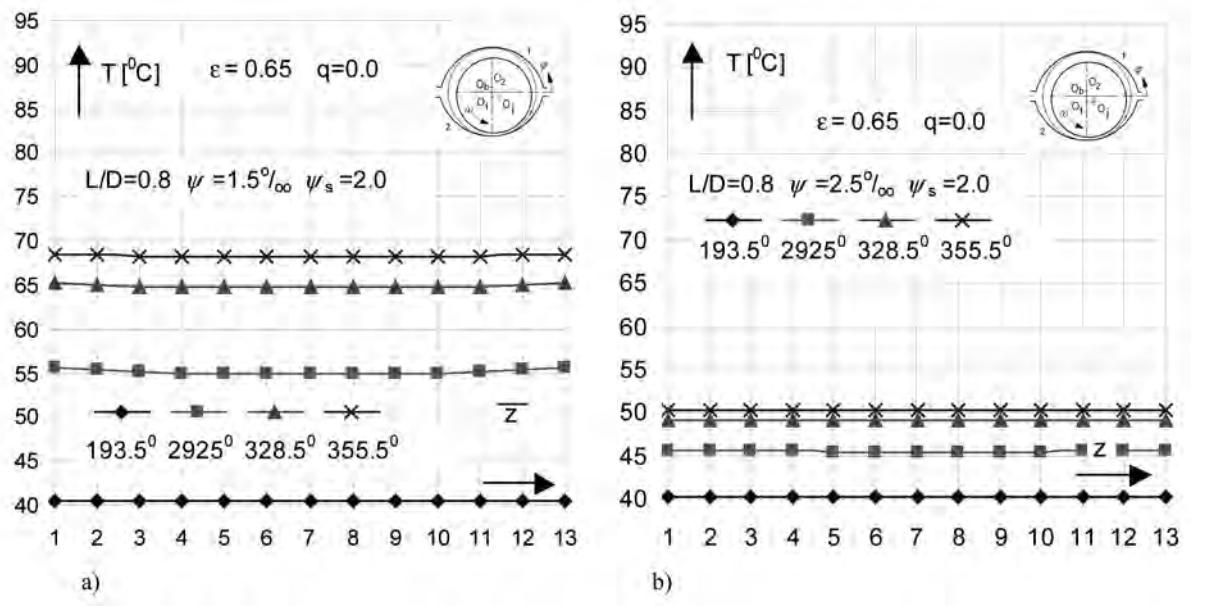

Fig. 10. Oil film temperature in axial cross-section at different bearing relative clearance and peripheral coordinates without misalignment: a) ψ = 1.5‰, b) ψ = 2.5‰

Rys. 10 Temperatura filmu smarowego w przekroju wzdłużnym dla różnego luzu łożyskowego i współrzędnych na obwodzie łożyska oraz współosiowych osi czopa i panewki: a) ψ = 1.5‰, b) ψ = 2.5‰

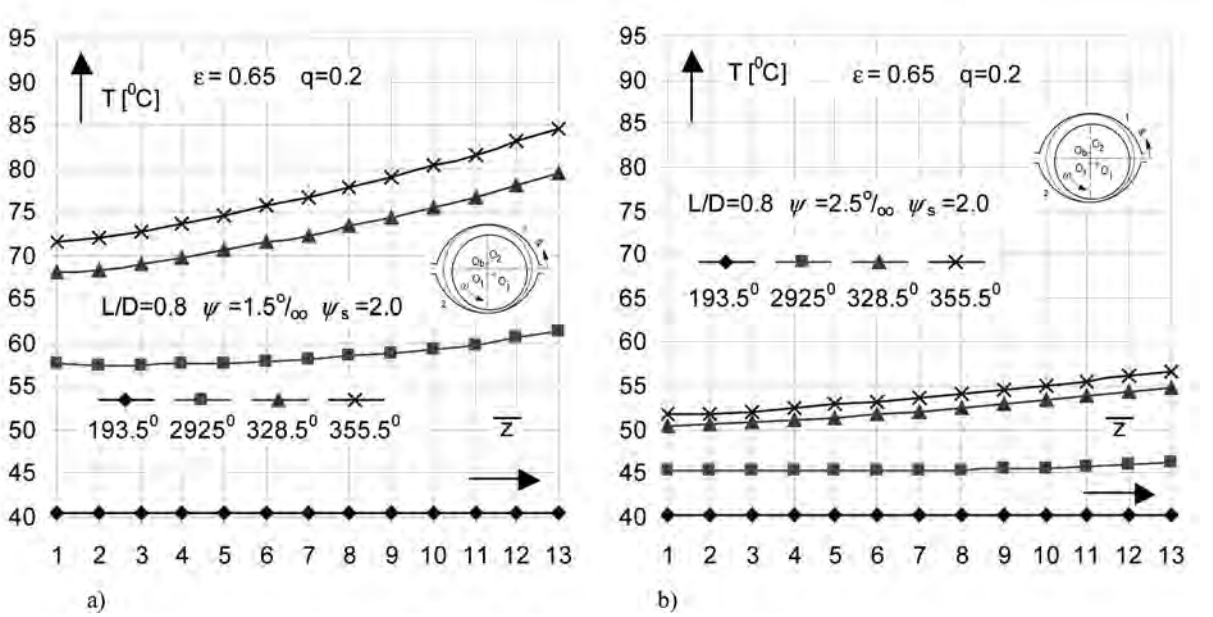

Fig. 11. Oil film temperature in axial cross-section at different bearing relative clearance and peripheral coordinates with misalignment: a) ψ = 1.5‰, b) ψ = 2.5‰

Rys. 11 Temperatura filmu smarowego w przekroju wzdłużnym dla różnego luzu łożyskowego i współrzędnych na obwodzie łożyska z niewspółosiowością osi czopa i panewki: a) ψ = 1.5‰, b) ψ = 2.5‰

An effect of misalignment on the axial temperature distribution at different peripheral coordinates is shown in **Fig. 12**, where a misalignment coefficient q = 0.1 causes an increase in the temperatures.

Figure 13 shows the maximum oil film temperature versus the Sommerfeld number on the upper and bottom lobe of bearing with the length to diameter ratio L/D = 1.0 and at misalignment coefficients q = 0.0 and q = 0.2, and the highest temperatures are observed on the lobe No. 2.

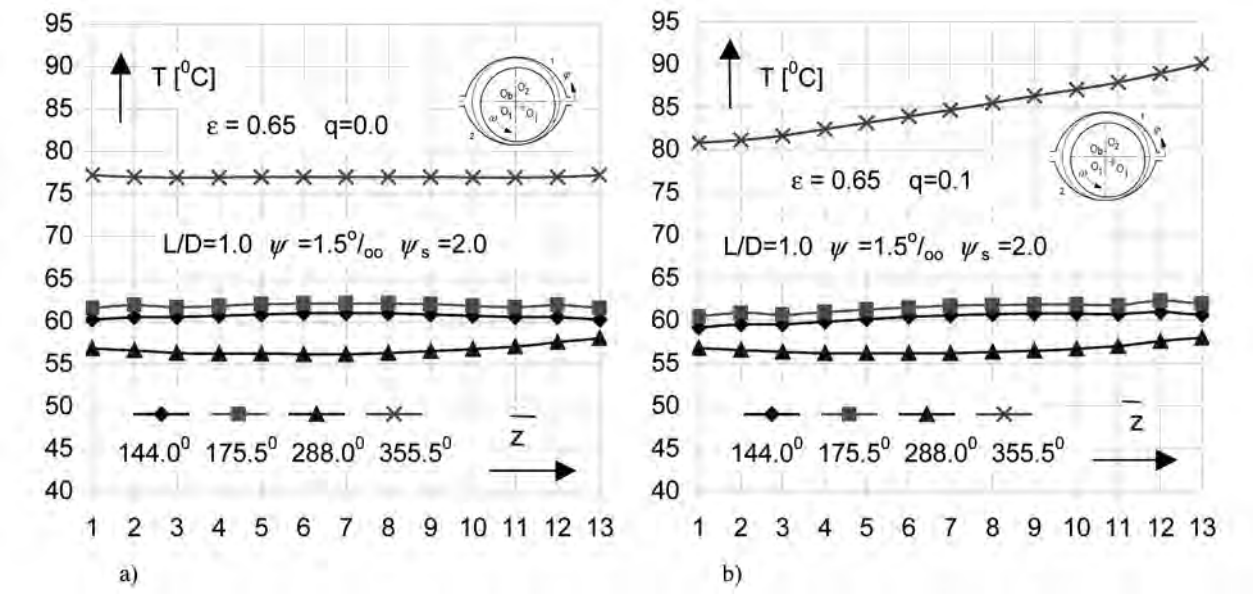

Fig. 12. Oil film temperature in axial cross-section at different peripheral coordinates: a) no misalignment, b) at assumed misalignment

Rys. 12 Temperatura filmu smarowego w przekroju wzdłużnym dla różnych współrzędnych na obwodzie łożyska: a) współosiowość, b) niewspółosiowość

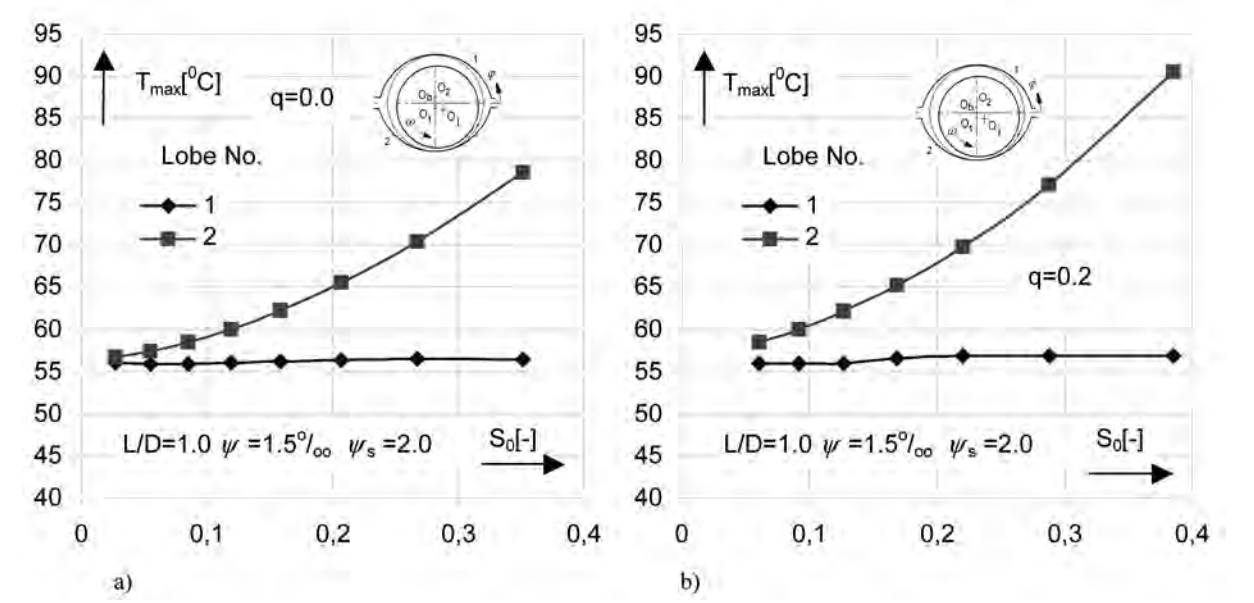

Fig. 13. Maximum oil film temperature on the lobes of bearing and at different values of misalignment: a) no misalignment, b) misalignment

Rys. 13 Maksymalna temperatura filmu smarowego na segmentach łożyska i dla różnych wartości przekoszenia: a) współosiowość, b) niewspółosiowość

The run of relative eccentricity (a) and static equilibrium position angles (b) versus the Sommerfeld number for different values of misalignment and at assumed value of relative eccentricity of journal ε are presented in **Fig. 14**, and there is an increase in the Sommerfeld number particularly at larger values of misalignment coefficient q (**Fig. 14a**). However, a smaller effect on the static equilibrium position angles α_{eq} is observed (**Fig. 14b**).

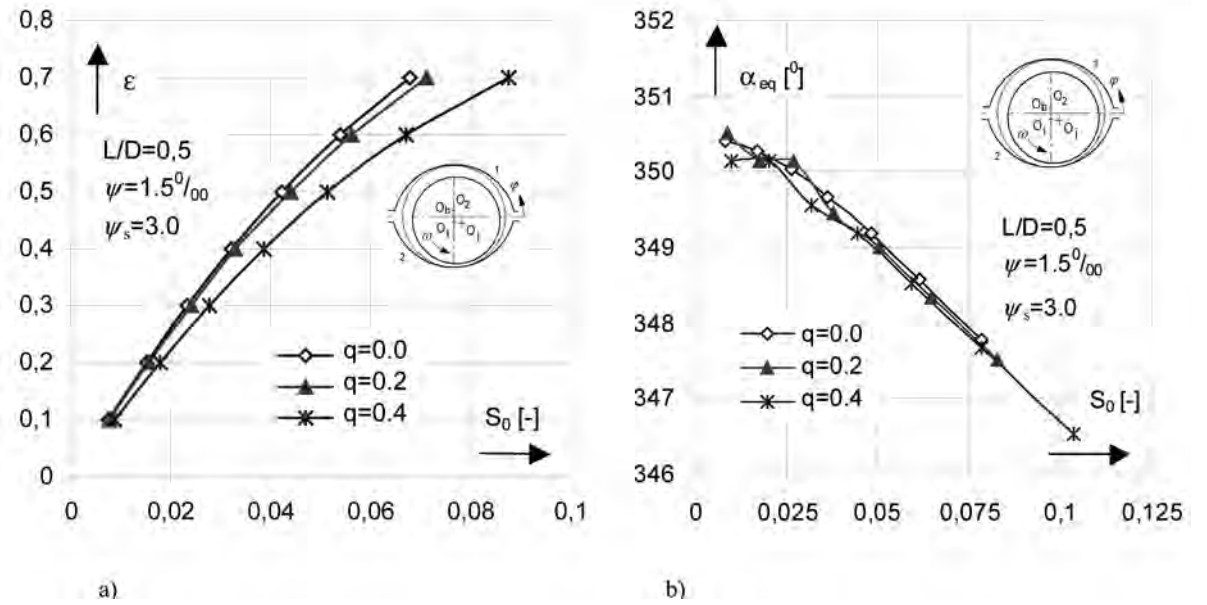

Fig. 14. Relative eccentricity (a) and static equilibrium position angles (b) versus the Sommerfeld number for different values of misalignment

Rys. 14 . Mimośrodowość względna (a) i kąt statycznego położenia równowagi (b) w funkcji liczby Sommerfelda dla różnych wartości współczynnika niewspółosiowości

Figure 15 shows the maximum oil film temperature for two values of bearing length to diameter ratio L/D = 0.5 and L/D = 1.0 as well as for different values of misalignment coefficient at the assumed value of bearing relative clearance and lobe relative clearance. The lowest temperatures are generated at the nil value of the misalignment coefficient (**Fig. 15a** and **Fig. 15b** see q = 0.0).

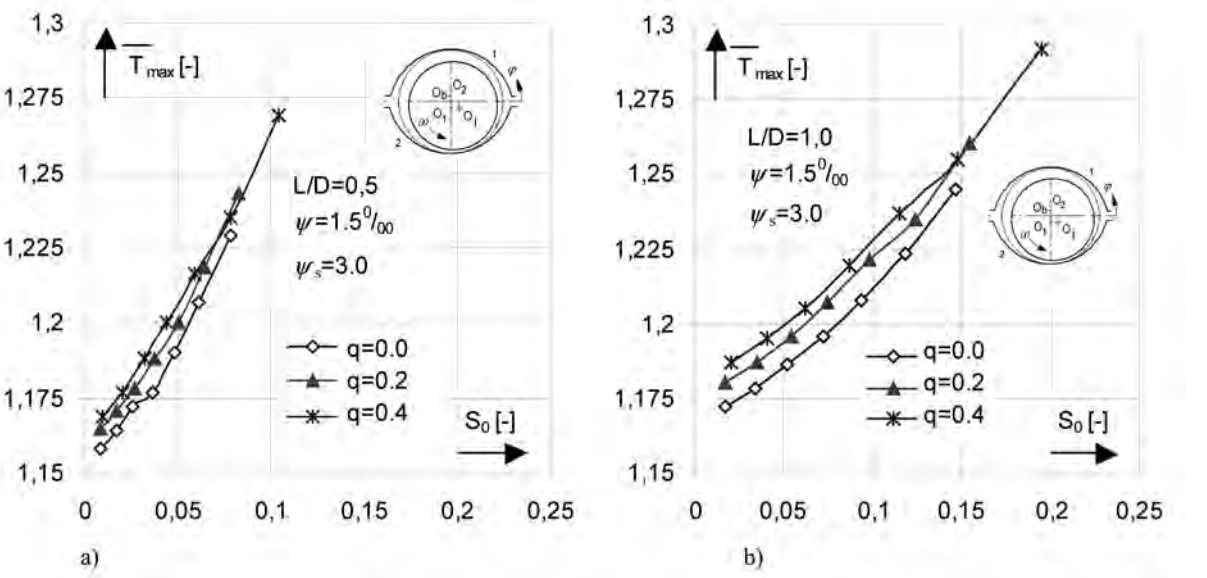

Fig. 15. Maximum oil film temperature for different values of bearing length to diameter ratio (a – for L/D = 0.5 and b – L/D = 1.0) and misalignment at assumed value of bearing relative clearance and lobe relative clearance

Rys. 15 Maksymalna temperatura filmu smarowego dla różnych wartości względnej długości łożyska (a – dla r L/D = 0,5 i b – L/D = 1,0) i współczynnika niewspółosiowości dla założonego luzu względnego i luzu względnego segmentu

An effect of the misalignment on the oil flow q_{flow} and power loss P_{loss} versus the Sommerfeld number is shown in **Fig. 16**. The oil flow is largest at the parallel axis of journal and sleeve (q = 0.0), and the smallest is at misalignment (**Fig. 16a**, e.g., q = 0.4). The power loss (**Fig. 16b**) shows the decrease for coefficients q = 0.1 and q = 0.2, but the increase in power loss is observed for larger values of misalignment coefficient q (**Fig. 16b**, e.g., q = 0.3 and q = 0.4) in full range of considered relative eccentricities.

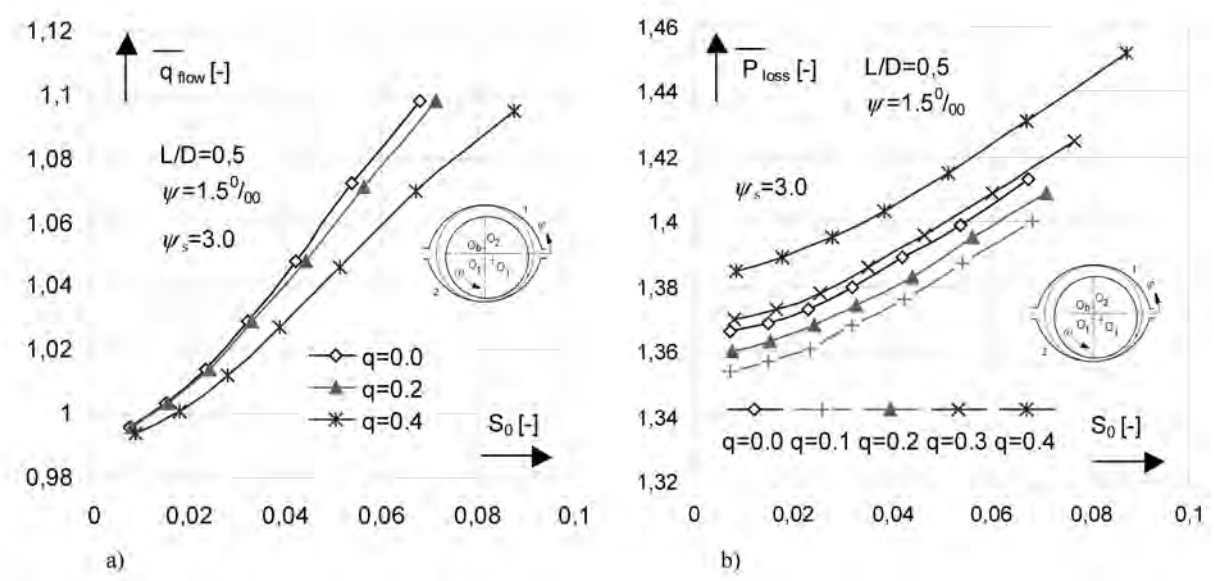

Fig. 16. Oil flow (a) and power loss (b) versus the Sommerfeld number for different values of misalignment
Rys. 16. Przepływ środka smarowego (a) i straty mocy (b) w funkcji liczby Sommerfelda dla różnych wartości współczynnika niewspółosiowości

An increase in the maximum oil film pressure, temperature, power loss that were obtained in **[L. 4, 8]** and in this paper by the author are also certified in the investigation in **[L. 10]**; however, they were carried out at flexible and compliant liners of the considered journal bearing.

FINAL REMARKS

The analysis of the real system of turbo unit journal bearings and the results of theoretical calculations that included an effect of misalignment allow for the following conclusions:

1. The misalignment affects the static characteristics of the bearing and particularly the value and position of maximum oil film pressure and temperature.
2. An increase of the misalignment of journal and bearing axis causes an increase in bearing maximum oil film pressure, temperature, oil flow, and power loss.
3. The operation of the bearing should be controlled for the maximum temperature on the bearing edges.
4. At assumed relative eccentricity of bearing, there is an increase in the Sommerfeld number at the increase of misalignment.
5. The control of turbine rotor vibration does not give enough information on the misalignment of the rotor and bearing axis and on the technical state of journal bearings.

The continuous improvement of the turbo unit efficiencies and the reduction of the costs of exploitation yield to higher rotor weights and consequently to enlarged specific bearing loads. Then, the journal bearings as the limiting factor for turbine design should be developed and calculated with the misalignment taken into account. Special means, such as the modification of axial cross-section of bearing, the flexible design of pedestals or textured liners, should decrease an effect of misalignment on the operation of bearing systems.

REFERENCES

1. Jang J.Y., Khonsari M.M.: On the Characteristics of Misaligned Journal Bearings. Lubricants 2015, 3, pp. 27–53.
2. Strzelecki S.: Problems of Reliability of the Turbounit Journal Bearings at Misaligned Axis of Journal and Sleeve. Proc. of the International Conference on the actual Problems of Reliability Technological, Power and Transporting Machines. Samara, Russia. 25–27 November 2003. Vol. 2. Part 1 and 2, 2003, pp. 233–239.
3. Abdou K.A., Saber E.: Effect of rotor misalignment on stability of journal bearings with finite width. Alexandria Engineering Journal. Alexandria University, 2020, pp. 3407– 3417.
4. Strzelecki S., Towarek Z.: Effect of journal misalignment on the oil film pressure and temperature distribution of 3-lobe offset journal bearing. Synopses of WTC 2005. World Tribology Congress III. 12–16 Sept. 2005. Washington D.C.
5. Strzelecki S.: The Load Capacity of Journal Bearing under effect of Axial Profile of Sleeve. First Mediterranean Tribology Conference, Jerusalem, 8–9 November 2000. Israel.
6. Mishra P.Ch., Thermal analysis of Elliptic Bore Journal; Bearing Considering the Effect of Shaft Misalignment. Japanese Society of Tribologists. Tribology Online 6, 5, 2011, pp. 239–246.
7. Gu T., Wang O.J., Xiong S., Liu Z., Gangopadhyay A., Liu Zh.: Profile Design for Misaligned Journal Bearings Subjected to Transient Mixed Lubrication. Journal of Tribology. 141 Issue 7, 2019.
8. Huber M., Strzelecki S., Steinhilper W., Sauer B.: Theoretical and Experimental Determination of the Performances of Misaligned and Statically Loaded Cylindrical Journal Bearings. Transaction of Mechanical Engineering. Vol. ME24, No. 1. The Institution of Engineers, Australia 2000, pp. 31–37.
9. Zhang X., Gu X.: Effect of misaligned bearing support performance on natural frequencies of marine propulsion shafting. Journal of Vibroengineering, Vol. 19, Issue 3, 2017, pp. 1854–1866.
10. Thomsen K., Klit P.: Improvement of journal bearing operation at heavy misalignment using bearing flexibility and compliant liners. Proc. ImechE. Part J: J. Engineering Tribology. 226(8), 2012, pp. 651–660.
11. Manser B., Belaidi I., Hamrani A., Khelladi S., Bakir F.: Performance of hydrodynamic journal bearing under the combined influence of textured surface and journal misalignment a numerical survey, https://hal.archives-ouvertes.fr/hal-02438009, 2020, pp. 1–33.
12. Jun S., Shaoyu Z., Yangyang F., Xiaoyong Z., Hu W., Qin T.: Effect of the axial movement of misaligned journal on the performance of hydrodynamic lubrication journal bearing with rough surface. Mechanics & Industry, Volume 20, Issue 4, 2019.
13. Zhang X., Gu X.: Effect of angular misalignment on the static characteristics of rotating externally pressurized air journal bearing. SCIENCE CHINA Technological Sciences. Vol. 62, Issue 9, 2019, pp. 1520–1533.
14. Jamali H.U., Al-Hammood A.: A New Method for the Analysis of Misaligned Journal Bearing. Tribology in Industry. Vol. 40, No. 2, 2018, pp. 2313–224.
15. Saridakis K.M., Nikolakopoulos P.G., Papadopoulos C.A.: Identification of wear and misalignment on journal bearings using artificial neural networks. Proc. Inst. of Mech. Engineers, Part J: Journal of Engineering Tribology. 226 issue 1, 2012, pp. 46–56.